


Stability analysis of the spin evolution fixed points in inspiraling compact binaries with black hole, neutron star, gravastar, or boson star components

Zoltán Keresztes[†] and László Árpád Gergely^{*}

Institute of Physics, University of Szeged, Dóm tér 9, Szeged 6720, Hungary

 (Received 8 August 2020; accepted 13 January 2021; published 13 April 2021)

Based on a recently derived secular spin evolution of black holes, neutron stars, gravastars, or boson stars in precessing compact binaries on eccentric orbit, we carry out a linear stability analysis of fixed point configurations. We identify the aligned and more generic coplanar configurations of the spins and orbital angular momentum as fixed points. Through a dynamical system analysis, we investigate their linear stability as function of the mass quadrupole parameter. Our most important results are as follows. Marginal stability holds for the binary configurations with both spins antialigned to the orbital angular momentum, for both spins aligned to the orbital angular momentum (with the exception of certain quadrupolar parameter ranges of neutron stars and boson stars), and for the extremal mass ratio. For equal masses, the configurations of one of the spins aligned and the other antialigned is stable for gravastar binaries, for neutron star binaries in the high quadrupolar parameter range, and for boson star binaries. For some unequal mass gravastar binaries, black hole binaries or neutron star binaries, a transition from stability to instability can occur during the inspiral, when one of the spins is aligned, while the other is antialigned to the orbital angular momentum. We also discover a transitional instability regime during the inspiral of certain gravastar, neutron star, or boson star binaries with opposing spins. For coplanar configurations we recover the marginally stable configurations leading to the libration phenomenon identified in previous numerical investigations lacking mass quadrupole contributions, and we analyze how it is affected by the quadrupolar structure of the sources. We also investigate the linear stability of black hole, neutron star, and boson star binaries, also of mixed black hole - gravastar, black hole - neutron star and black hole - boson star binaries. We find instabilities only for the gravastar - gravastar, boson star - boson star and black hole - boson star binaries. For a given spin configuration, marginal stability strongly depends on the value of the quadrupolar parameters. The stability region is larger for neutron star binaries than for black hole binaries, while the mixed systems have a restricted stability parameter region.

DOI: [10.1103/PhysRevD.103.084025](https://doi.org/10.1103/PhysRevD.103.084025)

I. INTRODUCTION

Compact binaries are among the most probable sources of gravitational radiation. All gravitational wave detections by the Advanced LIGO and Virgo detectors up to now have been from these type of sources, mostly from black hole - black hole systems [1,2] but also neutron star - neutron star [3] with multimessenger counterparts and a black hole - lighter compact object (which is either the lightest black hole or the heaviest neutron star yet discovered) [4].

Compact binary evolution can be well described analytically when the separation of the components is large as compared to their Schwarzschild radius. During this inspiral regime, the Keplerian evolution is modified by general relativistic corrections at first and higher post-Newtonian (PN) orders [5,6]. The spin of the compact objects also contributes at 1.5PN orders through the

spin-orbit (SO) and at 2PN orders through the spin-spin (SS) couplings [7–17]. The rotation of the compact object also induces a mass deformation, characterized by its quadrupole. The coupling of this to the mass of the other component enters at 2PN orders in the dynamics [18–21]. The 2PN order accurate instantaneous dynamics has been discussed in detail in Refs. [22–24]. Finally, gravitational radiation kicks in at 2.5PN orders [25].

In this paper, we continue the study of the secular spin dynamics in compact binaries on eccentric orbit during the inspiral regime on the conservative timescale, thus to 2PN order accuracy, commenced in our earlier work [26], which will be referred as Paper I. The binary components are compact objects with masses m_i , dimensionless spins χ_i , and quadrupolar parameter w_i spanning over a wide range of values, being 1 by definition for black holes, falling into $(-0.8, 1)$ for gravastars [27], into $(2, 14)$ for neutron stars [28,29], and into $(10, 150)$ for boson stars [30]. In Paper I, we have derived a closed system of first-order differential equations for the secular evolution of the spin polar angles

^{*}gergely@physx.u-szeged.hu

[†]zkeresztes@titan.physx.u-szeged.hu

κ_i (taken in the system with the orbital angular momentum \mathbf{L}_N on the z axis) and the difference of their azimuthal angles $\Delta\zeta$ (measured in the orbital plane).¹ We have analyzed both analytically and numerically various particular situations with special emphasis on the effect of the quadrupole parameter (thus on the role of the companion of a black hole) manifesting itself in the flip-flopping evolution of the polar angles. In this paper, we will concentrate on the stability analysis of fixed points of the spin angle dynamics, again emphasizing the role played by the quadrupole parameter.

The early analysis [11] of the orbit-averaged (secular) spin-precession equations for circular orbits, with only the SO and SS contributions included, identified four collinear spin and angular momentum equilibrium configurations (up-up, up-down, down-up, and down-down). Coplanar configurations representing equilibrium solutions of the instantaneous angular evolutions were also found [31]. There, a numerical study of the evolution of the phase shift (the difference in the azimuthal angles of the spins) revealed solutions librating about the equilibrium (interpreted as stable) and unstable solutions departing from the equilibrium. The latter appeared as a sequence of “long periods of stasis followed by short bursts of rapid divergence away from equilibrium,” dubbed as quasistable. Both these analyses disregarded the mass quadrupole–mass monopole contributions, driven by the parameters w_i .

When the rotation-induced quadrupole of black holes is also taken into account ($w_i = 1$), the four above-mentioned collinear configurations still represent equilibrium [21]. Among these, the up-down configuration was found unstable in certain parameter regimes [33].

In this paper, we revisit the analysis of the fixed points and their stability in the more generic context of compact binaries with black hole, neutron star, gravastar, or boson star components, thus allowing for an arbitrary value of the quadrupole parameters w_i .

In Sec. II, we sum up the closed system of evolution equations of the spin angles, and we establish the notations.

In Sec. III, we discuss this system from the dynamical systems point of view. We prove that the configurations of spins aligned and antialigned to the orbital angular momentum are still fixed points of the evolution in this more generic setup. We analyze their linear stability by deriving the marginal stability conditions. Then, we also discuss the equal and unequal mass configurations. For the former, we identify new types of instabilities, while for the latter, we

identify a new type of evolution during inspiral, encompassing a transitional instability.

We proceed with the analysis of the fixed points in Sec. IV, investigating coplanar configurations, discussing the dependence on the quadrupolar parameters of the marginally stable configurations. Further, we investigate here the linear stability of black hole, neutron star, and boson star binaries and also of mixed black hole - gravastar, black hole - neutron star, and black hole - boson star binaries.

In Sec. V, we present the conclusions.

II. SECULAR SPIN ANGLE EVOLUTIONS

The secular evolution of the spin angles κ_1 , κ_2 , and $\Delta\zeta \equiv \zeta_1 - \zeta_2$ has been derived in Paper I in the form of a closed first-order differential system,²

$$\frac{1}{R} \frac{d\kappa_1}{dt} = (1 + \nu - x_1 \cos \kappa_1 - \nu w_2 x_2 \cos \kappa_2) \times x_2 \sin \kappa_2 \sin \Delta\zeta, \quad (1)$$

$$\frac{1}{R} \frac{d\kappa_2}{dt} = -(1 + \nu^{-1} - x_2 \cos \kappa_2 - \nu^{-1} w_1 x_1 \cos \kappa_1) \times x_1 \sin \kappa_1 \sin \Delta\zeta, \quad (2)$$

$$\begin{aligned} \frac{1}{R} \frac{d\Delta\zeta}{dt} = & \nu - \nu^{-1} + (1 + 2\nu^{-1} - w_1 - w_1 \nu^{-1} x_1 \cos \kappa_1) x_1 \cos \kappa_1 \\ & - (1 + 2\nu - w_2 - w_2 \nu x_2 \cos \kappa_2) x_2 \cos \kappa_2 \\ & - (1 + \nu^{-1} - w_1 \nu^{-1} x_1 \cos \kappa_1) x_1 \cot \kappa_2 \sin \kappa_1 \cos \Delta\zeta \\ & + (1 + \nu - w_2 \nu x_2 \cos \kappa_2) x_2 \cot \kappa_1 \sin \kappa_2 \cos \Delta\zeta \\ & - x_1 x_2 \left(\frac{\sin \kappa_2}{\sin \kappa_1} - \frac{\sin \kappa_1}{\sin \kappa_2} \right) \cos \Delta\zeta, \end{aligned} \quad (3)$$

with the notations

$$R = \frac{3\eta\pi}{\mathfrak{I}_r^2}, \quad x_i = \frac{\chi_i}{\bar{\mathfrak{I}}_r}. \quad (4)$$

Here, $\nu = m_2/m_1 \leq 1$ is the mass ratio, and $\eta = \mu/m$ is the symmetric mass ratio (with $m = m_1 + m_2$ and $\mu = m_1 m_2 / m$ the total and reduced masses of the binary, respectively). Further, $\mathfrak{I}_r = c L_N / G m \mu$ is the dimensionless orbital angular momentum, and $\bar{\mathfrak{I}}_r$ is its average over a radial period (G , c , and L_N denoting the gravitational constant, the speed of light, and the magnitude of \mathbf{L}_N , respectively). Finally, \mathfrak{I} is the radial period expressed to 2 PN accuracy as Eq. (6) of Paper I. In addition, the derivatives are with respect to a dimensionless time variable $\mathfrak{t} = tc^3/Gm$ (with time t) introduced in Ref. [24].

²For notational simplicity, we omit the overbar (present in Paper I) from the secular time derivatives. We follow this simplified notation in what follows, keeping in mind that the equations describe secular dynamics.

¹If we were to use an alternative set of angular variables defined with the direction of the total orbital angular momentum \mathbf{L} , rather than the Newtonian angular momentum \mathbf{L}_N , differences would be induced only through the SO contribution to \mathbf{L} (as the PN and 2PN contributions lie in the direction of \mathbf{L}_N). For a discussion in terms of angles related to \mathbf{L} of the inspiral waveforms for the coplanar resonant configurations [31] and consequences in data analysis, see Ref. [32].

Note that $1/\bar{l}_r^2$ represents one relative PN order, as indicated by Eq. (8) of Ref. [24]. Hence, in the angular evolutions (1)–(3), the $\mathcal{O}(R)$, $\mathcal{O}(Rx_i)$, and $\mathcal{O}(Rx_ix_j)$ terms are PN, 1.5PN, and 2PN contributions, respectively.

III. COLLINEAR SPIN ORIENTATIONS: LINEAR STABILITY ANALYSIS

The closed system (1)–(3) becomes ill behaved for the aligned configurations $\sin \kappa_i = 0$. This is the usual singularity of the polar angle in a spherical system of coordinates, for which the azimuthal angles ζ_i become ill defined.

The case when only one of $\sin \kappa_i$ evolves through zero is discussed in Appendix B of Paper I. We showed that, despite the apparent coordinate singularity, the system passes through such a configuration driven by a well-defined dynamics.

When both $\sin \kappa_1$ and $\sin \kappa_2$ vanish, the spins remain parallel or antiparallel to the orbital angular momentum, i.e., the angles κ_i being constant,³ as can be seen from Eqs. (1) and (2). With these the aligned configurations fulfill the conditions for the fixed points of the spin dynamics. Remarkably, all terms containing the problematic angles ζ_i in the evolution equations of the Euler angles vanish; thus, their dynamics remains well defined. We proceed with the linear stability analysis of these aligned configurations.

We denote the fixed points as $\kappa_{(0)i}$ and the points obtained by a slight deviation $\epsilon_i \delta \kappa_i(\mathbf{t})$ as

$$\kappa_i(\mathbf{t}) = \kappa_{(0)i} + \epsilon_i \delta \kappa_i(\mathbf{t}), \quad (5)$$

with $\epsilon_i = \cos \kappa_{(0)i}$ representing a sign (this choice ensures that the perturbed angle stays in the domain $[0, \pi]$). To leading order, the closed system becomes

$$\frac{d\Delta\zeta}{dt} = A + \left(B_1 \frac{\delta\kappa_2}{\delta\kappa_1} - B_2 \frac{\delta\kappa_1}{\delta\kappa_2} \right) \cos \Delta\zeta, \quad (6)$$

$$\frac{d\delta\kappa_1}{dt} = B_1 \delta\kappa_2 \sin \Delta\zeta, \quad (7)$$

$$\frac{d\delta\kappa_2}{dt} = -B_2 \delta\kappa_1 \sin \Delta\zeta, \quad (8)$$

with the constants defined as

$$\begin{aligned} \frac{A}{R} &= \nu - \nu^{-1} + \epsilon_1(1 + 2\nu^{-1} - w_1 - \epsilon_1\nu^{-1}w_1x_1)x_1 \\ &\quad - \epsilon_2(1 + 2\nu - w_2 - \epsilon_2\nu w_2x_2)x_2, \\ \frac{B_1}{R} &= [\epsilon_1(1 + \nu - \epsilon_2\nu w_2x_2) - x_1]x_2, \\ \frac{B_2}{R} &= [\epsilon_2(1 + \nu^{-1} - \epsilon_1\nu^{-1}w_1x_1) - x_2]x_1. \end{aligned} \quad (9)$$

³A similar conclusion valid only for black holes ($w_i = 1$) also emerges from Eqs. (3.2a) and (3.2b) of Ref. [21].

Time derivatives of Eqs. (6)–(8) combined lead to the simple second-order differential equation

$$\frac{d^2\mathcal{Z}}{dt^2} + (A^2 + 4B_1B_2)\mathcal{Z} = 0 \quad (10)$$

in the variable

$$\mathcal{Z} = \delta\kappa_1\delta\kappa_2 \sin \Delta\zeta, \quad (11)$$

with independent solutions $\mathcal{Z}_{\pm} = e^{\pm i\Omega t}$, where $\Omega^2 \equiv 4B_1B_2 + A^2$. Obviously, for $\Omega^2 \leq 0$, there is a runaway solution, and the fixed point is unstable, whereas for $\Omega^2 > 0$, the independent solutions become harmonic functions, which could be combined into

$$\mathcal{Z} = Q \cos(\Omega t + G), \quad (12)$$

with Q and G constants.

Then, Eq. (7) becomes

$$\begin{aligned} \frac{d(\delta\kappa_1)^2}{dt} &= 2B_1\delta\kappa_1\delta\kappa_2 \sin \Delta\zeta \\ &= 2B_1Q \cos(\Omega t + G), \end{aligned} \quad (13)$$

which results in

$$(\delta\kappa_1)^2 = F_1 + \frac{2B_1Q}{\Omega} \sin(\Omega t + G), \quad (14)$$

with another integration constant $F_1 \geq |2B_1Q/\Omega|$. Similarly,

$$(\delta\kappa_2)^2 = F_2 - \frac{2B_2Q}{\Omega} \sin(\Omega t + G), \quad (15)$$

with the integration constant $F_2 \geq |2B_2Q/\Omega|$. The solutions (14) and (15) prove that the aligned configurations $\sin \kappa_{1,2} = 0$ are marginally stable for $\Omega^2 > 0$.

A. Sufficient conditions for marginal stability

The above stability criterion depends on seven parameters:

$$\nu, \quad x_i, \quad w_i, \quad \epsilon_i. \quad (16)$$

We discuss their possible ranges below. The mass ratio is $\nu \in (0, 1]$. The value of \bar{l}_r can be estimated by Eq. (8) of Ref. [24], which for not too eccentric bound orbits is of the order $\bar{l}_r \geq 1/\sqrt{\bar{e}}$ (equality holds for circular orbits [24]). Assuming $\chi_i \leq 1$ and that the PN approximation is valid for the PN parameter $\bar{e} \in (0, 0.1)$ gives for circular orbits $x_i = \chi_i/\bar{l}_r \in (0, 0.3)$.

First, we note that the positivity of B_i implies

$$\epsilon_1\epsilon_2w_{3-i} < \epsilon_1\epsilon_2 \frac{1 + \nu^{2i-3}(1 - \epsilon_ix_i)}{\epsilon_{3-i}x_{3-i}}. \quad (17)$$

TABLE I. The positivity conditions for B_1 and B_2 . A sufficient condition for marginal stability is met when their signs agree.

	$B_1 > 0$	$B_2 > 0$
$\kappa_{(0)1} = 0$	$w_2 < W_2^-$	$w_1 < W_1^-$
$\kappa_{(0)2} = 0$		
$\kappa_{(0)1} = 0$	Always	$w_1 > W_1^+$
$\kappa_{(0)2} = \pi$		
$\kappa_{(0)1} = \pi$	$w_2 > W_2^+$	Always
$\kappa_{(0)2} = 0$		
$\kappa_{(0)1} = \pi$	Never	Never
$\kappa_{(0)2} = \pi$		

The signs of B_1 and B_2 are shown in Table I. There, we introduced the notations

$$W_i^\pm = \frac{1 + \nu^{3-2i}(1 \pm x_{3-i})}{x_i}, \quad (18)$$

which for the allowed parameter ranges are bound as

$$\begin{aligned} W_1^- &> \frac{10}{3}, & W_2^- &> \frac{17}{3}, \\ W_1^+ &> \frac{10}{3}, & W_2^+ &> \frac{20}{3}. \end{aligned} \quad (19)$$

Note that as $\bar{\Gamma}_r^{-1}$ increases monotonically during the inspiral the derivatives

$$\frac{dW_i^\pm}{d(\bar{\Gamma}_r^{-1})} = -\frac{1 + \nu^{3-2i}}{\chi_i} \bar{\Gamma}_r^2 < 0 \quad (20)$$

ensure that the functions W_i^\pm decrease monotonically.

For extreme mass ratios $\nu \ll 1$, we immediately obtain $|B_1 B_2| \ll A^2$, resulting in $\Omega^2 > 0$, and thus the fixed point of the system is marginally stable. In addition, for $B_1 B_2 > 0$, the system is also marginally stable.

Finally, there is marginal stability also in the case when at least one the B_i vanishes, unless $A = 0$ also holds. When both spins are nonvanishing, this occurs for the pair of quadrupolar parameters

$$w_i = \frac{1 + \nu^{3-2i}(1 - \epsilon_{3-i} x_{3-i})}{\epsilon_i x_i} \in \{\pm W_i^\pm\}, \quad (21)$$

among which only $w_i \in \{W_i^\pm\}$ are admitted on physical grounds. Note that the vanishing of B_i and A also implies the vanishing of B_{3-i} . Hence, in order to have marginal stability, both B_i cannot vanish simultaneously.

If only one spin is present,

$$\begin{aligned} x_{3-i} &= 0 \\ w_i &= \frac{\nu^{3-2i} - \nu^{2i-3} + \epsilon_i(1 + 2\nu^{2i-3})x_i}{(\epsilon_i + \nu^{2i-3}x_i)x_i}. \end{aligned} \quad (22)$$

Note that in this case $\Omega^2 = A^2$ is a convex function, everywhere positive outside its double degenerate root w_i , which represents its minimum.

For equal masses, Eq. (22) reduces to

$$\begin{aligned} x_{3-i} &= 0 \\ w_i &= \frac{3}{1 + \epsilon_i x_i}. \end{aligned} \quad (23)$$

There are the following cases to be discussed:

- (i) When both spins are antialigned with the orbital angular momentum, the system is marginally stable. All other aligned configurations require additional conditions to be imposed on the parameters.
- (ii) In the configuration of the compact binary components with both spins aligned, $w_1 < 10/3$ together with $w_2 < 17/3$ implies $w_i < W_i^-$ during the whole inspiral; hence, marginal stability holds for all mass ratios and spin values. Therefore, the aligned black hole - black hole, gravastar - gravastar, and black hole - gravastar binary systems are marginally stable.
- (iii) For neutron star binaries with both spins aligned, the marginal stability depends on their equation of state. For low w_i values, both $B_i \geq 0$ and $B_{3-i} > 0$ could hold true throughout the inspiral, in this case the system being marginally stable. Similarly, marginal stability could hold throughout the inspiral for larger values of w of either aligned neutron star binaries or aligned boson star binaries, when both $B_i \leq 0$ and $B_{3-i} < 0$ hold. There could be cases when marginal stability during the initial phases of the inspiral turns into instability and possibly turns back to stability again, or initial instability turns into marginal stability, as W_i^- evolve during the inspiral.
- (iv) With one spin aligned and another antialigned, the marginal stability criterion is $w_i > W_i^+$ for the aligned spin. This could hold either during the whole inspiral or only at its latter stages, when the decreasing W_i^+ may slide below a high enough value of the quadrupolar parameter w_i , even if it does not hold in the earlier stages of the inspiral.

B. Equal masses

For equal masses,

$$\begin{aligned} \frac{\Omega^2}{R^2} &= \sum_{i=1}^2 [(1 + x_i^2)w_i^2 - 6w_i + 9 + 2\epsilon_i w_i(w_i - 3)x_i]x_i^2 \\ &+ 2(2 + w_1 w_2)x_1^2 x_2^2 - \sum_{i=1}^2 2\epsilon_i(4 + w_j + w_i w_j)x_i x_j^2 \\ &- 2\epsilon_1 \epsilon_2 x_1 x_2 \left[1 + w_1 w_2 - \sum_{i=1}^2 (3 + 2x_i^2)w_i \right]. \end{aligned} \quad (24)$$

1. Equal spins and quadrupolar parameters

Equation (24) reduces for $w_1 = w_2 = w$ and $x_1 = x_2 = x = \chi/\bar{\Gamma}_r$ to

$$\begin{aligned} \frac{\Omega^2}{R^2} = & 2[(3-w)^2 + 2(1+w^2)x^2]x^2 \\ & - 2\epsilon_1\epsilon_2(1-6w+w^2-4wx^2)x^2 \\ & - 8(\epsilon_1 + \epsilon_2)(1+w)x^3. \end{aligned} \quad (25)$$

For $\epsilon_1 = \epsilon_2 = \epsilon$, Eq. (25) reduces to

$$\frac{\Omega^2}{R^2} = 4x^2(x + wx - 2\epsilon)^2, \quad (26)$$

and Ω^2 vanishes for

$$w = w_{cr_1} = \frac{2\epsilon}{x} - 1, \quad (27)$$

but apart from this critical value, it is always positive, and thus the configuration is marginally stable. Then:

- (a) For $\epsilon = -1$, $w_{cr_1} < -1$, which is outside of the astrophysically interesting range. The configuration with both spins antialigned to the orbital angular momentum is marginally stable.
- (b) For $\epsilon = 1$,

$$\frac{dw_{cr_1}}{d(\bar{\Gamma}_r^{-1})} = -\frac{2}{\chi}\bar{\Gamma}_r^2 < 0 \quad (28)$$

shows that w_{cr_1} decreases monotonically during the inspiral, attaining its minimal value at the end of it. The lowest value occurs at the end of the inspiral on circular orbits, leading to the bound $w_{cr_1} > 17/3$. Thus, the critical value may fall into the possible range of the quadrupole parameter for neutron stars and boson stars. Apart from this value, the configuration with both spins aligned to the orbital angular momentum is marginally stable.

- (c) For $\epsilon_1\epsilon_2 = -1$,

$$\frac{\Omega^2}{R^2} = 4x^2(w-1)(w+wx^2-x^2-5) \quad (29)$$

and Ω^2 has two roots:

$$w_- = 1, \quad w_+ = 1 + \frac{4}{x^2+1} \in (4.7, 5). \quad (30)$$

The angular frequency $\Omega^2 > 0$ for $w > w_+$ and $w < 1$, and $\Omega^2 < 0$ for $1 < w < w_+$. Hence, for the configurations with one spin aligned and another antialigned to the orbital angular momentum, gravastar binaries are marginally stable, while black hole binaries are unstable. For neutron star binaries, these configurations

can be either unstable or marginally stable (depending on the equation of state), while for boson star binaries, they are always marginally stable. These findings are compatible with and expand those described under iv) in Sec. III A for the case of equal masses, spins, and quadrupole parameters.

2. Second spin negligible

In another limiting case, $x_2 \ll x_1$, the expression (24) reduces to

$$\frac{\Omega^2}{R^2} = x_1^2(3 - w_1 - \epsilon_1 w_1 x_1)^2, \quad (31)$$

which is positive, thus yielding marginal stability, except for

$$w_1 = w_{cr_2}^{\epsilon_1} = \frac{3}{1 + \epsilon_1 x_1}, \quad (32)$$

which reproduces the earlier result (23). Thus, there is a critical value of w_1 as a function of x_1 where the configuration becomes unstable. The critical value ranges as $w_{cr_2} \in (2.3, 3)$ for $\epsilon_1 = 1$ and as $w_{cr_2} \in (3, 4.3)$ for $\epsilon_1 = -1$. Both can emerge only in a neutron star binary.

C. Nonequal masses in the nonextreme mass ratio regime

For simplicity, we set $w_1 = w_2 = w$ and $x_1 = x_2 = x$. Then, the configurations with $\epsilon_1 = \epsilon_2$ are marginally stable. Indeed, when both spins are counterrotating, $\epsilon_1 = \epsilon_2 = -1$, and this has been already analytically proven in a more generic context (see item i) in Sec. III A), while for the corotating case, $\epsilon_1 = \epsilon_2 = 1$, the stability condition reads

$$\begin{aligned} \frac{\Omega^2}{R^2} = & 4(2 + \nu + \nu^{-1})(1-x)(1-wx)x^2 \\ & + 4(1-w)^2x^4 + (\nu - \nu^{-1})^2(1-2x+wx^2)^2 > 0. \end{aligned} \quad (33)$$

There are no real roots of the equation $\Omega^2 = 0$, and numerical analysis has proven that these configurations are marginally stable. We illustrate this for $x = 0.3$ on Fig. 1.

The cases $\epsilon_1 = -\epsilon_2$ are shown on Fig. 2, for the mass ratio $\nu = 0.9$. The blue domain represents $\Omega^2 < 0$, thus unstable configurations, while in the yellow area, $\Omega^2 > 0$. For values of w not shown on the figures [$w > 8$ (left panel) and $w > 25$ (right panel)], $\Omega^2 > 0$ holds (with the exception of the continuation of the red curve), and hence marginal stability occurs.

The green horizontal lines on the panels represent black hole binaries. The configuration with the larger mass black hole spin aligned to the orbital angular momentum and the smaller mass black hole antialigned ($\epsilon_1 = 1$, $\epsilon_2 = -1$) is

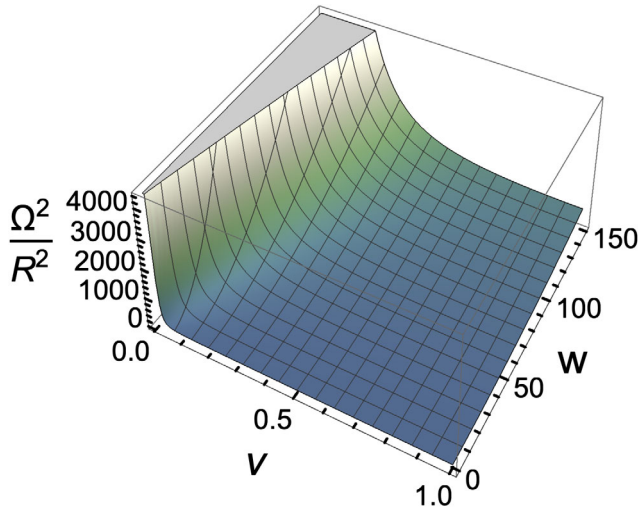


FIG. 1. Marginal stability generically holds in the nonequal mass case with both spins aligned to the orbital angular momentum, irrespective of the values of ν , w (shown) and x (represented for $x = 0.3$).

initially marginally stable, becoming unstable as the inspiral orbit shrinks, as found in Ref. [33].

For neutron star binaries in the quadrupole parameter range $w \in (2, 4)$, linear stability can disappear abruptly during the inspiral for any of the $(\epsilon_1 = 1, \epsilon_2 = -1)$ and $(\epsilon_1 = -1, \epsilon_2 = 1)$ configurations, similarly to the black hole binaries.

By contrast, neutron star binaries with $w > 4$ in the $(\epsilon_1 = 1, \epsilon_2 = -1)$ configuration are always marginally stable.

There are also configurations allowing for a sequence of evolutions, which are stable, then unstable, then stable again during the inspiral. In these cases, the instability is only transitional. Such systems are:

- (A) the gravastar binaries with w values in the lower part of their allowed range, in the configuration $(\epsilon_1 = 1, \epsilon_2 = -1)$;
- (B) neutron star binaries with w values in the higher part of their allowed range, in the $(\epsilon_1 = -1, \epsilon_2 = 1)$ configuration;
- (C) boson star binaries, also in the $(\epsilon_1 = -1, \epsilon_2 = 1)$ configuration. For the latter, the instability occurs only for a very limited part of the evolution (across the red curve in the right panel of Fig. 2).

Finally note that the location and extension of the blue domain depends on the mass ratio.

We discuss the marginal stability for other mass ratio values below. For

$$\epsilon_2 = -\epsilon_1, \quad w_1 = w_2 = w, \quad x_1 = x_2 = x, \quad (34)$$

stability is determined by the sign of

$$\begin{aligned} \frac{\Omega^2}{R^2} = & (\nu - \nu^{-1})^2 + [2 - w(\nu + \nu^{-1})]^2 x^4 \\ & + 4\epsilon_1(\nu - \nu^{-1})(1 + \nu + \nu^{-1} - w)(1 + wx^2)x \\ & - 4\epsilon_1(\nu - \nu^{-1})(1 + w)x^3 + 2[2w^2 \\ & + 2(\nu^2 + \nu + 1 + \nu^{-1} + \nu^{-2}) \\ & + w(\nu^2 - 4\nu - 6 - 4\nu^{-1} + \nu^{-2})]x^2. \end{aligned} \quad (35)$$

The roots of the $\Omega^2 = 0$ equation are

$$w_{\pm}^{(\epsilon_1, \epsilon_2 = -\epsilon_1)} = \frac{U_1 + \epsilon_1 U_2 \pm V \sqrt{1 + \epsilon_1 x(\nu^{-1} - \nu)}}{W_1 + \epsilon_1 W_2} \quad (36)$$

with

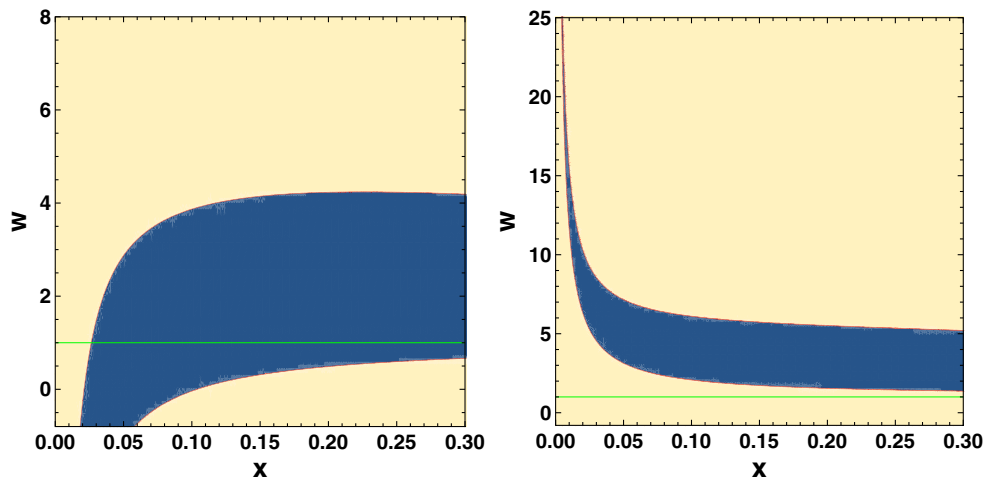


FIG. 2. Marginal stability regions for the quadrupolar parameter w represented by positive Ω^2 (shown in yellow) as opposed to instability regions (blue) for $\epsilon_1 = 1, \epsilon_2 = -1$ (left panel) and $\epsilon_1 = -1, \epsilon_2 = 1$ (right panel). The horizontal green lines are for black hole binaries. Various transitions from stability to instability and back to stability are possible as the inspiral proceeds (with increasing PN parameter and x).

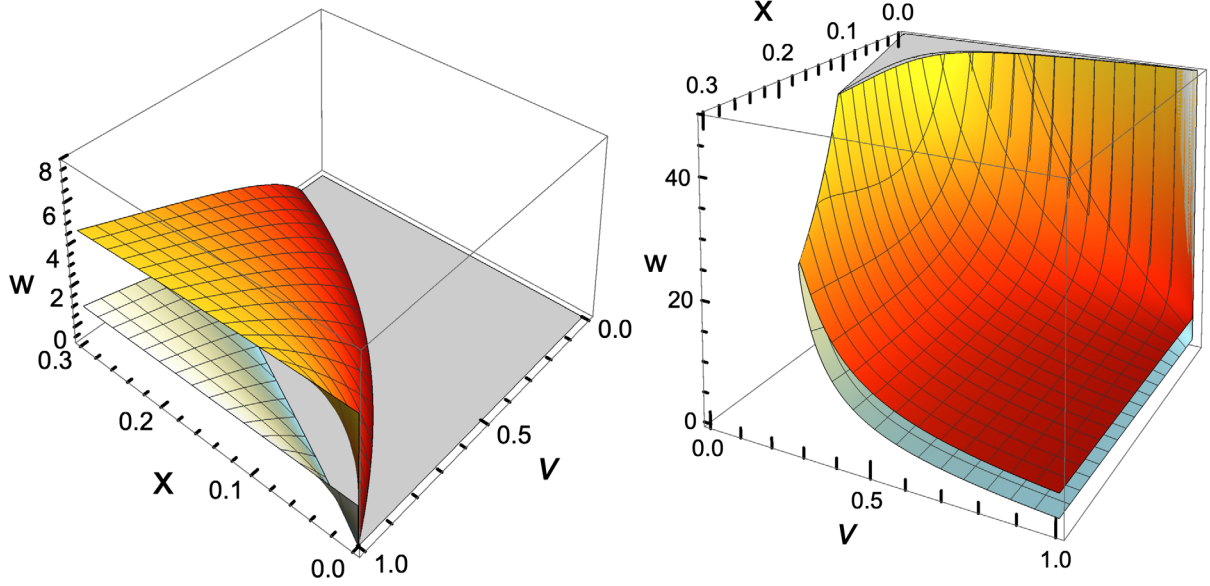


FIG. 3. Marginal stability regions for the quadrupolar parameter w represented by positive Ω^2 regions lying outside the two surfaces $\Omega^2 = 0$, for $\epsilon_1 = 1, \epsilon_2 = -1$ (left panel) and $\epsilon_1 = -1, \epsilon_2 = 1$ (right panel). Marginal stability generically holds for low mass ratios ν , while for higher values of ν , regions of stability and instability alternate, depending on the value of the quadrupolar parameter w .

$$\begin{aligned}
 U_1 &= [-1 + 4\nu + 6\nu^2 + 4\nu^3 - \nu^4 + 2x^2\nu(1 + \nu^2)]x, \\
 U_2 &= -2\nu(1 - \nu^2) + 2(1 - \nu^4)x^2, \\
 V &= 2\nu[(1 + \nu)^2 - \epsilon_1(1 - \nu^2)x]x, \\
 W_1 &= [4\nu^2 + (1 + \nu^2)^2x^2]x, \\
 W_2 &= 4\nu(1 - \nu^2)x^2.
 \end{aligned} \tag{37}$$

The two $\Omega^2 = 0$ surfaces are represented on Fig. 3 (left panel for $\epsilon_1 = 1$ and right panel for $\epsilon_1 = -1$). In the region between the surfaces $\Omega^2 < 0$, they are unstable regions. For lower values of ν , either there are no real roots, hence no $\Omega^2 = 0$ surfaces [for $\epsilon_1 = -1$, this happens below $\nu = (\sqrt{4x^2 + 1} - 1)/2x$], or the roots are outside the physically allowed region for the quadrupolar parameter (for $\epsilon_1 = 1$); thus, marginal stability holds irrespective of the value of w . For larger values of ν , a similar structure of the stability and instability regions as for $\nu = 0.9$ emerges, with the lower stability region possibly missing for certain parameter combinations.

IV. COPLANAR SPIN ORIENTATION: FIXED POINTS AND LINEAR STABILITY ANALYSIS

There are additional fixed points of the system (1)–(3) given by

$$\frac{d\kappa_i}{dt} = 0, \quad \frac{d\Delta\zeta}{dt} = 0. \tag{38}$$

The first condition is satisfied for $i = 1$ and $i = 2$, respectively, with

$$0 = (1 + \nu - x_1 \cos \kappa_1 - \nu w_2 x_2 \cos \kappa_2) x_2 \sin \kappa_2 \sin \Delta\zeta \tag{39}$$

and

$$0 = (1 + \nu^{-1} - x_2 \cos \kappa_2 - \nu^{-1} w_1 x_1 \cos \kappa_1) x_1 \sin \kappa_1 \sin \Delta\zeta, \tag{40}$$

while the second one is satisfied with

$$\begin{aligned}
 0 &= \nu - \nu^{-1} + (1 + 2\nu^{-1} - w_1 - \nu^{-1} w_1 x_1 \cos \kappa_1) x_1 \cos \kappa_1 \\
 &\quad - (1 + 2\nu - w_2 - \nu w_2 x_2 \cos \kappa_2) x_2 \cos \kappa_2 \\
 &\quad - (1 + \nu^{-1} - \nu^{-1} w_1 x_1 \cos \kappa_1) x_1 \cot \kappa_2 \sin \kappa_1 \cos \Delta\zeta \\
 &\quad + (1 + \nu - \nu w_2 x_2 \cos \kappa_2) x_2 \cot \kappa_1 \sin \kappa_2 \cos \Delta\zeta \\
 &\quad - x_1 x_2 \left(\frac{\sin \kappa_2}{\sin \kappa_1} - \frac{\sin \kappa_1}{\sin \kappa_2} \right) \cos \Delta\zeta.
 \end{aligned} \tag{41}$$

To investigate the stability about the fixed point $(\kappa_{(0)1}, \kappa_{(0)2}, \Delta\zeta_{(0)})$ under the perturbations of the angles, we parametrize them as

$$\kappa_1(t) = \kappa_{(0)1} + \delta\kappa_1(t), \tag{42}$$

$$\kappa_2(t) = \kappa_{(0)2} + \delta\kappa_2(t), \tag{43}$$

$$\Delta\zeta(t) = \Delta\zeta_{(0)} + \delta\Delta\zeta(t). \tag{44}$$

The perturbations $|\delta\kappa_1|$, $|\delta\kappa_2|$, and $|\delta\Delta\zeta|$ are initially much smaller than 1, and if they stay so, the configuration is stable or marginally stable. Equations (39) and (40) are solved by $\sin \kappa_{1,2} = 0$ or $\sin \Delta\zeta = 0$. The first condition

represents collinear spin configurations discussed earlier, while the second yields the coplanar case. In this latter case, Eq. (41) reduces to the constraint

$$\begin{aligned}
0 = & \nu - \nu^{-1} + (1 + 2\nu^{-1} - w_1 - \nu^{-1}w_1x_1 \cos\kappa_{(0)1})x_1 \cos\kappa_{(0)1} \\
& - (1 + 2\nu - w_2 - \nu w_2x_2 \cos\kappa_{(0)2})x_2 \cos\kappa_{(0)2} \\
& - \epsilon_{\Delta\zeta}(1 + \nu^{-1} - \nu^{-1}w_1x_1 \cos\kappa_{(0)1})x_1 \cot\kappa_{(0)2} \sin\kappa_{(0)1} \\
& + \epsilon_{\Delta\zeta}(1 + \nu - \nu w_2x_2 \cos\kappa_{(0)2})x_2 \cot\kappa_{(0)1} \sin\kappa_{(0)2} \\
& - \epsilon_{\Delta\zeta}x_1x_2 \left(\frac{\sin\kappa_{(0)2}}{\sin\kappa_{(0)1}} - \frac{\sin\kappa_{(0)1}}{\sin\kappa_{(0)2}} \right) \quad (45)
\end{aligned}$$

between $\kappa_{(0)1}$ and $\kappa_{(0)2}$, where $\epsilon_{\Delta\zeta} = \pm 1$ represents the sign of $\cos\Delta\zeta_{(0)}$. The simplest case of $\nu = 1$, $w_1 = w_2$, and $x_1 = x_2$ is solved for $\kappa_{(0)1} = \kappa_{(0)2}$.

To linear order in the perturbations about the fixed point, the evolution equations (1)–(3) give

$$\frac{d\delta\kappa_1}{dt} = A_1\delta\Delta\zeta, \quad (46)$$

$$\frac{d\delta\kappa_2}{dt} = -A_2\delta\Delta\zeta, \quad (47)$$

$$\frac{d\delta\Delta\zeta}{dt} = A_3\delta\kappa_1 - A_4\delta\kappa_2, \quad (48)$$

with

$$\frac{A_1}{R} = (1 + \nu - x_1 \cos\kappa_{(0)1} - \nu w_2x_2 \cos\bar{\kappa}_2)x_2 \sin\bar{\kappa}_2, \quad (49)$$

$$\begin{aligned}
\frac{A_3}{R} = & -(1 + 2\nu^{-1} - w_1 - 2\nu^{-1}w_1x_1 \cos\kappa_{(0)1})x_1 \sin\kappa_{(0)1} \\
& - \epsilon_{\Delta\zeta}(1 + \nu^{-1})x_1 \cot\kappa_{(0)2} \cos\kappa_{(0)1} \\
& + \epsilon_{\Delta\zeta}\nu^{-1}w_1x_1^2 \cot\kappa_{(0)2} \cos 2\kappa_{(0)1} \\
& - \epsilon_{\Delta\zeta}(1 + \nu - \nu w_2x_2 \cos\kappa_{(0)2})x_2 \frac{\sin\kappa_{(0)2}}{\sin^2\kappa_{(0)1}} \\
& + \epsilon_{\Delta\zeta}x_1x_2 \frac{\cos\bar{\kappa}_1(\sin^2\kappa_{(0)1} + \sin^2\kappa_{(0)2})}{\sin^2\kappa_{(0)1} \sin\kappa_{(0)2}}. \quad (50)
\end{aligned}$$

The additional constants A_2 and A_4 are obtained from A_1 and A_3 , respectively, with the changes $1 \leftrightarrow 2$ and $\nu \rightarrow \nu^{-1}$. From this system, a second-order decoupled differential equation for $\delta\Delta\zeta$ can be derived as

$$\frac{d^2\delta\Delta\zeta}{dt^2} = (A_1A_3 + A_2A_4)\delta\Delta\zeta. \quad (51)$$

For $\omega^2 \equiv -(A_2A_4 + A_1A_3) > 0$, the evolutions of $\delta\Delta\zeta$, $\delta\kappa_1$, and $\delta\kappa_2$ are described by harmonic functions yielding marginally stable fixed points. (In the terminology of Ref. [31], the configuration is stable when $\Delta\zeta$ evolves

through a harmonic function about the equilibrium configuration.) Deviations from such marginally stable configurations generate the librations.

Fixed points with $\omega^2 \leq 0$ are unstable. The sign of ω^2 depends on the parameters

$$\nu, \quad x_i, \quad w_i, \quad \kappa_{(0)i}, \quad \epsilon_{\Delta\zeta}, \quad (52)$$

which are subject to the constraint (45).

A. Early inspiral limit

At sufficiently large separations, where $w_1x_1/\nu \ll 1$ and $\nu w_2x_2 \ll 1$ hold, ω^2 reduces to

$$\begin{aligned}
\frac{\bar{\Gamma}_r^2\omega^2}{R^2} = & [3(2 + \nu^{-1} + \nu) - (1 + \nu)w_1 \\
& - (1 + \nu^{-1})w_2]\chi_1\chi_2 \sin\kappa_{(0)1} \sin\kappa_{(0)2} \\
& + 2\epsilon_{\Delta\zeta}(2 + \nu^{-1} + \nu)\chi_1\chi_2 \cos\kappa_{(0)1} \cos\kappa_{(0)2} \\
& + \epsilon_{\Delta\zeta}(1 + \nu^{-1})^2\chi_1^2 \frac{\sin^2\kappa_{(0)1}}{\sin^2\kappa_{(0)2}} + \epsilon_{\Delta\zeta}(1 + \nu)^2\chi_2^2 \frac{\sin^2\kappa_{(0)2}}{\sin^2\kappa_{(0)1}}. \quad (53)
\end{aligned}$$

Note that $\bar{\Gamma}_r^2$ has factored out. For $\chi_2/\chi_1 \ll 1$, there is stability for $\Delta\zeta_{(0)} = 0$ and instability for $\Delta\zeta_{(0)} = \pi$. For generic spins, but $w_1 = w_2 = w$ and $\text{sgn}(\kappa_{(0)1}) = \text{sgn}(\kappa_{(0)2})$, there is stability for $\Delta\zeta_{(0)} = 0$ if $w \leq 3$ (including gravastars, black holes, and some of the neutron stars) and instability for $\Delta\zeta_{(0)} = \pi$ if $w \geq 3$ (the complementary set of neutron stars and boson stars).

B. Numerical investigation for high spins

The stability of coplanar fixed points emerging as solutions of the constraint (45) depends on the sign of ω^2 . Both the location and number of fixed points and their stability depend severely on the parameters (52). By fixing ν , x_i , w_i , and $\epsilon_{\Delta\zeta}$, the constraint (45) reduces to curves in the parameter plane of spin polar angles $\kappa_{(0)i}$.

Instead of x_i we may also fix the spin magnitudes χ_i , but then $\bar{\Gamma}_r$ emerges as a third parameter. We represent then the constraint as contour curves of constant $\bar{\Gamma}_r$ in the parameter plane $(\kappa_{(0)1}, \kappa_{(0)2})$.

By Eq. (8) of Ref. [24] to leading order, $\bar{\Gamma}_r^2 = (1 - \bar{e}_r^2)/\bar{e}$. For $\bar{e} < 0.1$, on circular orbits, $\bar{\Gamma}_r > 3$. For a nonvanishing eccentricity, $\bar{e}_r^2 < 0.75$, the limit $\bar{\Gamma}_r > 2$ still holds. We do not discuss higher eccentricities, as gravitational radiation is supposed to consume it efficiently toward the end of the inspiral. This implies that in Figs. 4–7 we will visualize contour curves for $\bar{\Gamma}_r > 2$ only.

For Fig. 4, $\Delta\zeta_{(0)} = 0$, $\chi_i = 1$, and $\nu \approx 0.82$ were chosen. The first panel, representing gravastar binaries with $w_i = 0$

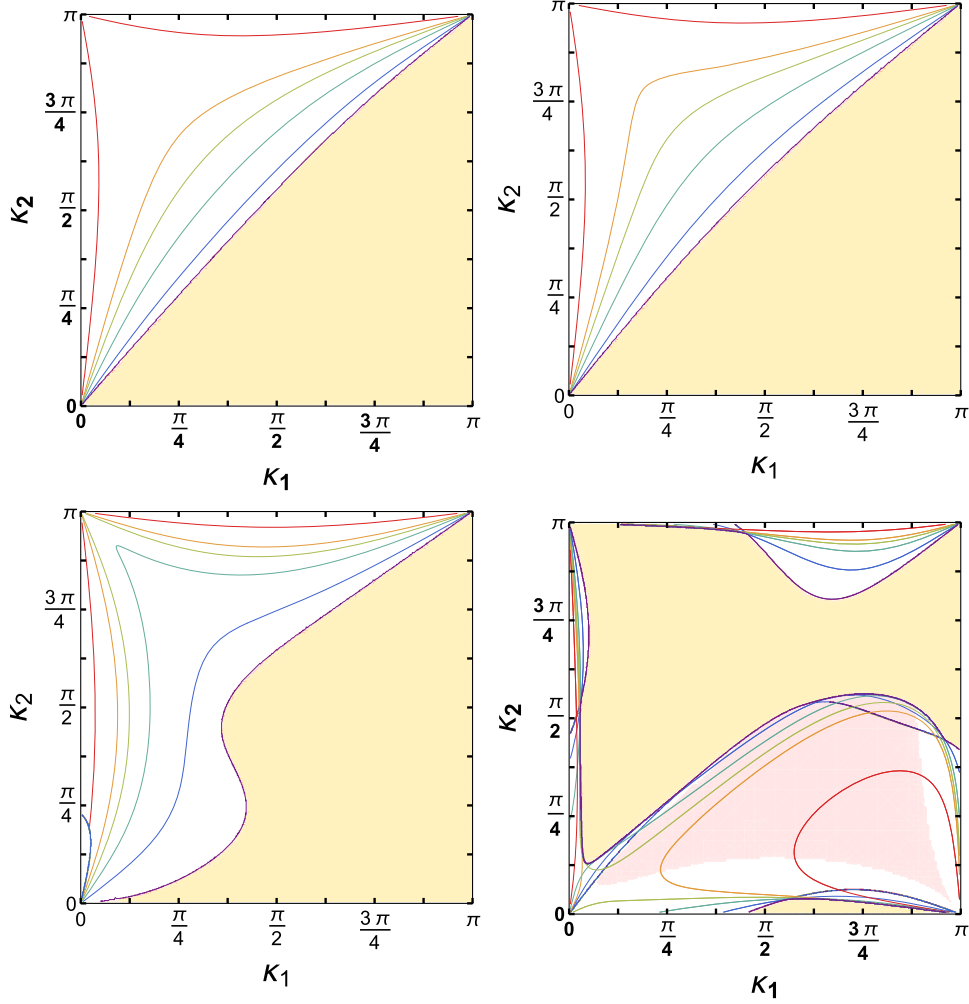


FIG. 4. Linear stability of the coplanar fixed-point configurations with $\Delta\zeta_{(0)} = 0$ as function of $\kappa_{(0)1}$ and $\kappa_{(0)2}$, represented for $\chi_i = 1$ and $\nu \approx 0.82$. White regions are marginally stable, and pastel pink are unstable. Yellow regions do not have fixed points. The purple, blue, green, olive, orange, and red contour lines refer to the 2, 4, 8, 12, 16, and 40 values of \bar{l}_r , respectively. The panels show binaries composed of gravastar - gravastar with $w_i = 0$ (top left), black hole - black hole with $w_i = 1$ (top right), neutron star - neutron star with $m_{NS_1} = 1.7 M_\odot$, $w_{NS_1} = 2.55$, $m_{NS_2} = 1.4 M_\odot$, $w_{NS_2} = 4.3$ (bottom left), and boson star - boson star with $w_{BS_1} = 17$, $w_{BS_2} = 22$, respectively.

reproduces the contour lines from Fig. 2 of Ref. [31], where the mass quadrupole was disregarded. The purple, blue, green, olive, orange, and red contour lines emerge for the values 2 (0.5), 4 (1), 8 (2), 12 (3), 16 (4), and 40 of \bar{l}_r . The numbers in brackets (where applicable) are the corresponding L_N , given for easier comparison with Fig. 2 of Ref. [31]. In the white region, the fixed points are marginally stable (with any deviation leading to libration), while in the yellow area, there are no fixed points (the deviations increase monotonically). The second panel represents black hole binaries, i.e., $w_i = 1$, with the same color codes and contour lines. They are slightly deformed as compared to the gravastar binary. The third panel represents a neutron star - neutron star binary with masses $m_{NS_1} = 1.7 M_\odot$ and $m_{NS_2} = 1.4 M_\odot$. According to Table VII of Ref. [28], the respective quadrupole parameters of the neutron stars with

a FPS (Friedman-Pandharipande + Skyrme) equation of state are $w_{NS_1} = 2.55$ and $w_{NS_2} = 4.3$. The fourth panel represents a boson star - boson star binary with quadrupole parameters $w_{BS_1} = 17$ and $w_{BS_2} = 22$. These quadrupole parameters roughly correspond to the values on the bottom two curves of Fig. 4 in Ref. [30] at $\chi_i = 1$. These two curves represent a system with mass ratio $\nu = 0.82$, as on our figure. The contour lines of \bar{l}_r cross each other in certain regions for the boson star - boson star system. However, this is no problem, as the crossing lines correspond to different values of \bar{l}_r and thus to distinct phases of the inspiral. It is clear from a comparison of the four panels that the contour lines of \bar{l}_r depend significantly on the quadrupole parameter. They run on a white background, representing the parameter regions with linear stability. The red patch on the fourth panel represents the unstable

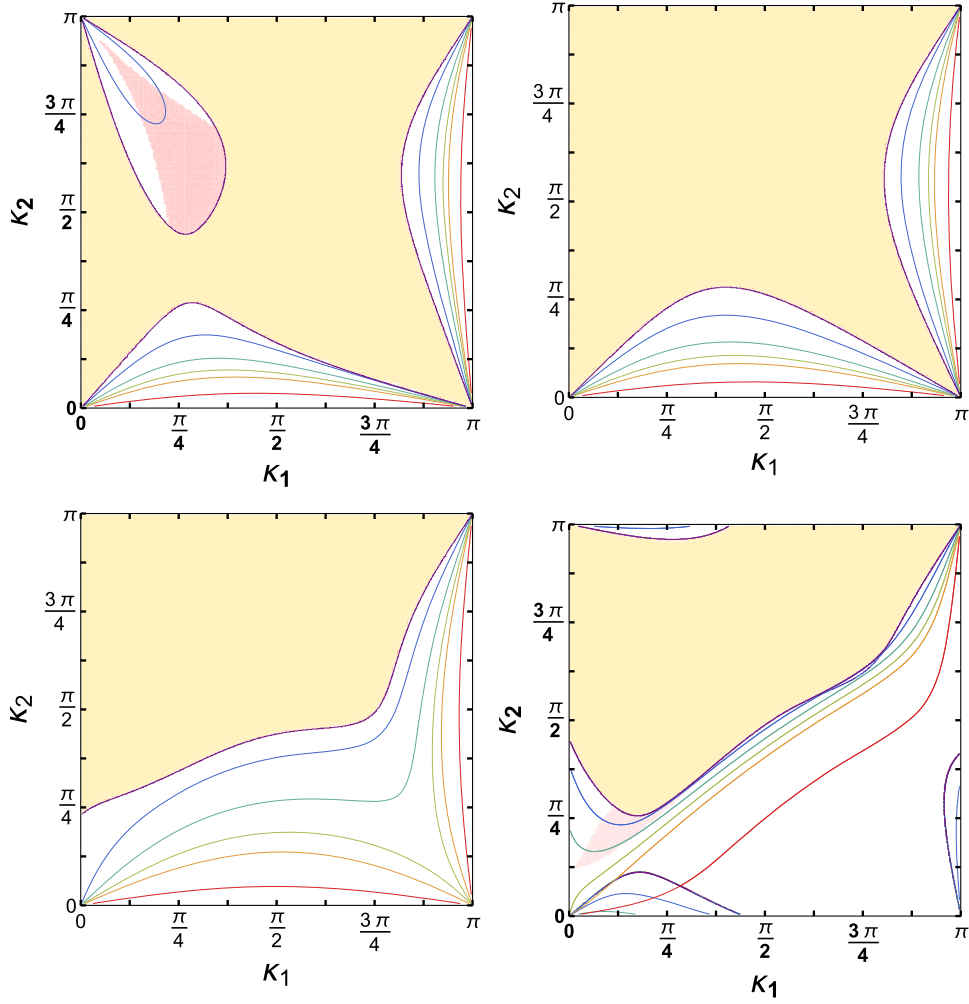


FIG. 5. Linear stability analysis for the coplanar configuration with $\Delta\zeta_{(0)} = \pi$. The panels and color codes are identical to those of Fig. 4.

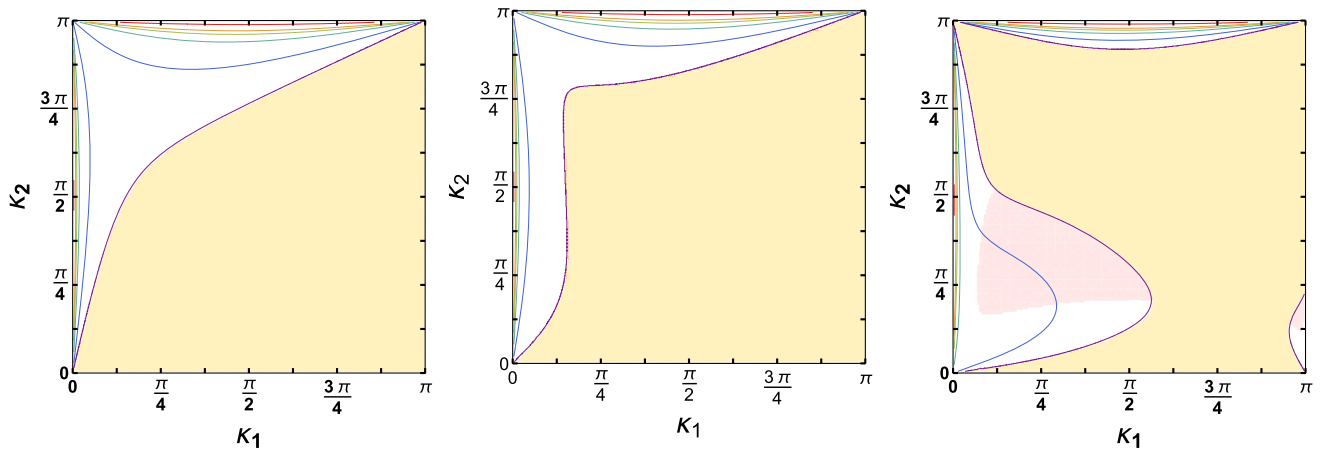


FIG. 6. Linear stability of the coplanar fixed-point configurations with $\Delta\zeta_{(0)} = 0$ as function of $\kappa_{(0)1}$ and $\kappa_{(0)2}$, represented for $\chi_i = 1$ and $\nu \approx 0.82$. White regions are marginally stable, and pastel pink are unstable. Yellow regions do not have fixed points. The purple, blue, green, olive, orange, and red contour lines refer to the 2, 4, 8, 12, 16, and 40 values of \tilde{l}_r , respectively. The panels show binaries composed of black hole - gravastar with $w_{GS} = 0$ (left), black hole - neutron star with $m_{NS} = 1.4 M_\odot$, $w_{NS} = 4.3$ (middle), and black hole - boson star with $w_{BS} = 17$, respectively.

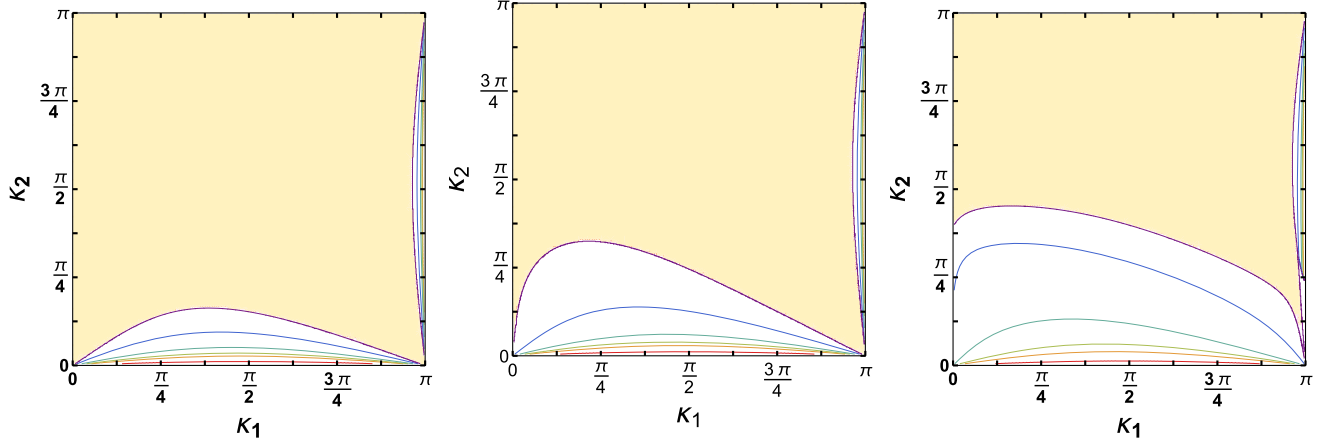


FIG. 7. Linear stability analysis for the coplanar configuration with $\Delta\zeta_{(0)} = \pi$. The panels and color codes are identical to those of Fig. 6.

parameter region. Note the contour lines which extend on both stable and unstable regions. On the yellow background, there are no fixed points.

In the four panels of Fig. 5, the contour lines for all four above-mentioned binary systems are shown for $\Delta\zeta_{(0)} = \pi$, all other parameters identical. In this case, the value of the quadrupole parameter affects even more the stability analysis. Unstable regions appear both for the gravastar - gravastar and boson star - boson star binaries. The stability region is much larger for neutron stars than black holes. Overlapping contour curves appear only for the boson star binaries.

The regions which contain unstable patches embedded in a linearly stable region deserve additional investigation. We have checked numerically that whenever linear stability holds in these regions generic nonlinear perturbations confirm the stability up to perturbations of 0.5% but can destroy stability if the perturbation is roughly larger than 1%. This happens as second- and higher-order perturbative effects become important. This feature is in agreement with the analysis of Ref. [31] intended to be performed for black holes, but as the mass quadrupole was disregarded, they rather hold for gravastars with $w_i = 0$).

In Fig. 6, $\Delta\zeta_{(0)} = 0$, $\chi_i = 1$, and $\nu \approx 0.28$ were chosen. The first, second, and third panels represent black hole - gravastar, black hole - neutron star, and black hole - boson star binaries, respectively. The quadrupole parameters for the gravastar, neutrons star, and boson star are $w_{GS} = 0$, $w_{NS} = 4.3$ (corresponding to the mass $m_{NS} = 1.4 M_\odot$) and $w_{BS} = 17$. These systems are also visualized in Fig. 7 for $\Delta\zeta_{(0)} = \pi$. As a generic rule, the stability regions are smaller than for binaries of identical nature.

V. CONCLUSIONS

In this paper, we investigated the closed system of first-order differential equations for the spin orientations derived in Paper I from the dynamical system analysis point of

view, by performing a linear stability analysis of the evolutions of spin polar angles and the difference of their azimuthal angles.

By investigating a sufficient condition of stability:

- (i) systems with both spins antialigned with the orbital angular momentum were found marginally stable.
- (ii) systems of black hole - black hole, gravastar - gravastar, and black hole - gravastar binaries with both spins aligned with the orbital angular momentum were also found marginally stable. Binaries with neutron star and boson star components and aligned spins could be marginally stable in various stages of the inspiral depending on how their quadrupolar parameter compares to the functions W_i^- which decrease monotonically during the inspiral.
- (iii) in the configurations with one spin aligned and another antialigned, marginal stability could hold either during the whole inspiral for sufficiently large values of w_i or only at the latter stages of the inspiral.

In the analysis of the case of equal masses, spins, and quadrupole parameters, we investigated a necessary condition for marginal stability. This has resulted in:

- (a) the confirmation of our earlier finding that the configurations with the spins antialigned to the orbital angular momentum are marginally stable.
- (b) the aligned configurations also turned out marginally stable, with the exception of a critical quadrupolar parameter value allowed for neutron stars and boson stars only.
- (c) for black holes and gravastars, the configurations with one spin aligned and another antialigned to the orbital angular momentum being found unstable. For neutron stars, these configurations were found either marginally stable or unstable (depending on the equation of state), while for boson stars they turned out marginally stable.

TABLE II. Summary of results on marginal stability (+) or instability (−) of the collinear spin configurations in compact binary systems (B) composed of gravastars (GS), black holes (BH), neutron stars (NS), and boson stars (BS) for various mass ratios $\nu = m_2/m_1 \leq 1$ and spin orientations. The first spin in the name of a binary (for example BBH $\downarrow\uparrow$) refers to the higher mass component. The stability may be different for lower values (low) or higher values (hiw) of the allowed quadrupolar parameter range [$w_i \in (-0.8, 1)$ for GS, $w_i = 1$ for BH, $w_i \in (2, 14)$ for NS, and $w_i \in (10, 150)$ for BS]. For example, BNS $\uparrow\downarrow$ low denotes a binary system of neutron stars with the spin of the more (less) massive neutron star parallel (antiparallel) to the Newtonian angular momentum \mathbf{L}_N and with quadrupolar parameter in the lower range $w \gtrsim 2$.

$\uparrow L_N$	$\uparrow S_1 \uparrow S_2$	$\uparrow S_i \downarrow S_{j \neq i}$	$\downarrow S_1 \downarrow S_2$
$\nu \ll 1$	+	+	+
$\nu \lesssim 1, \chi_1 = \chi_2 = \chi,$ $w_1 = w_2 = w$	+ (illustrated for $x \equiv \frac{z}{l} = 0.3$ in Fig. 1)	+ (BGS $\downarrow\uparrow$, BBH $\downarrow\uparrow$, BNS $\uparrow\downarrow$ hiw, BBS $\uparrow\downarrow$) Evolves during the inspiral as +- (BGS $\uparrow\downarrow$ hiw, BBH $\uparrow\downarrow$, BNS $\uparrow\downarrow$ low, BNS $\downarrow\uparrow$ low) Evolves during the inspiral as + - + (BGS $\uparrow\downarrow$ low, BNS $\downarrow\uparrow$ hiw, BBS $\downarrow\uparrow$) (shown for $\nu = 0.9$ in Fig. 2, for arbitrary ν in Fig. 3)	+
$\nu = 1, \chi_1 = \chi_2 = \chi,$ $w_1 = w_2 = w$	+ for BGS, BBH + for BNS and BBS if $w \neq w_{cr1}$, where $w_{cr1} = \frac{2}{x} - 1 > \frac{17}{3}$ decreases during the inspiral	+ for BGS, BBS + for BNS with $w > w_+$, where $w_+ \equiv 1 + \frac{4}{x^2+1} \in (4.7, 5)$ decreases during the inspiral - for BBH, BNS with $w < w_+$	+
Sufficient conditions in all other cases	+ for BGS, BBH, GS-BH + for BNS with $w_1 < \frac{10}{3}, w_2 < \frac{17}{3}$ + for BNS or BBS with $w_i \leq W_1^-$ and $w_{3-i} < W_{3-i}^-$ or with $w_i \geq W_1^-$ and $w_2 > W_2^-$, where W_i^- decrease during inspiral according to Eq. (18), bound as $W_1^- > \frac{10}{3}, W_2^- > \frac{17}{3}$	+ for binaries with a NS or BS as the i^{th} component, obeying $w_i > W_i^+$, where W_i^+ decrease during inspiral according to Eq. (18), bound as $W_1^+ > \frac{10}{3}, W_2^+ > \frac{20}{3}$	+

These results generalize the stability analysis result performed earlier for black hole binaries (which had the mass quadrupolar contributions neglected, hence rather holding for gravastars with $w_i = 0$).

For nonequal masses, we found that marginal stability occurs for all values of the quadrupolar parameter (for gravastars, black holes, neutron stars, or boson stars in binary configurations) when both spins are either anti-aligned or aligned to the orbital angular momentum. Other cases were represented in Fig. 2.

For black hole binaries, we recovered the transition from stability to instability during the inspiral occurring when the spin of the larger black hole is aligned to the orbital angular momentum and that of the smaller mass black hole is antialigned, discussed in Ref. [33]. In the opposite alignment case, the evolution was marginally stable.

We identified similar evolutions leading to the abrupt disappearance of stability for neutron star binaries in the quadrupole parameter range $w \in (2, 4)$. Contrary to black hole binaries, this can happen if any of the neutron star spins is aligned to the orbital angular momentum, while the

other is antialigned. Neutron star binaries with $w > 4$, with the larger mass neutron star spin aligned to the orbital angular momentum, are always marginally stable.

We also identified configurations allowing for a sequence of evolutions, which are stable, then unstable, then stable again during the inspiral. In the following cases, a transitional instability occurs:

- (A) gravastar binaries with w values in the lower part of their allowed range, in the configuration of the larger mass gravastar spin aligned to the orbital angular momentum;
- (B) neutron star binaries with w values in the higher part of their allowed range, with the smaller mass neutron star spin aligned to the orbital angular momentum;
- (C) boson star binaries, also in the configuration of the smaller mass boson star spin aligned to the orbital angular momentum (in this case, the instability occurs only for a brief part of the evolution).

We summarize these results in Table II.

Marginal stability holds generically, when one of the spins is collinear with the Newtonian angular momentum

TABLE III. Marginal stability (+) holds generically, when one of the spins is collinear with the Newtonian angular momentum \mathbf{L}_N , while the second spin is negligible, with the single exception of a particular value of the quadrupolar parameter of a spinning neutron star (NS) or boson star (BS) in a binary with $\nu \lesssim 1$.

$\uparrow L_N$	$\uparrow S_1$	$\downarrow S_1$
$\nu = 1, \chi_2 = 0$	+ for all type of binaries, unless m_1 is a NS with $w_1 = w_{cr2}^+ = \frac{3}{1+\chi_1} \in (2.3, 3)$	+ for all type of binaries, unless m_1 is a NS with $w_1 = w_{cr2}^- = \frac{3}{1-\chi_1} \in (3, 4.3)$
$\nu \lesssim 1, \chi_2 = 0$	+ for all type of binaries, unless m_1 is a NS or BS with $w_1 = \frac{(1+2\nu^{-1})\chi_1 - (\nu^{-1}-\nu)}{(\nu^{-1}\chi_1+1)\chi_1} \leq w_{cr2}^+$	+ for all type of binaries, unless m_1 is a NS or BS with $w_1 = -\frac{(1+2\nu^{-1})\chi_1 + (\nu^{-1}-\nu)}{(\nu^{-1}\chi_1-1)\chi_1} \geq w_{cr2}^-$
$\nu \ll 1, \chi_2 = 0$	+ for all type of binaries, (no instability in the physical range of w_1)	+ for all type of binaries, (no instability in the physical range of w_1)

TABLE IV. Regions with marginal stability (+), instability (-), and with no fixed points (/) of a given spin configuration (κ_1, κ_2) in the coplanar cases $\Delta\zeta = 0, \pi$ for various binaries. For each binary, the pair (κ_1, κ_2) refers to a particular phase of the inspiral represented by the corresponding level curve in Figs. 4–7.

(κ_1, κ_2)	$\Delta\zeta$	GSB	BHB	NSB	BSB	BH-GS	BH-NS	BH-BS
$(\frac{3\pi}{8}, \frac{\pi}{4})$	0	/	/	+	-	/	/	-
	π	/	+	+	+	/	+	+
$(\frac{3\pi}{8}, \frac{3\pi}{4})$	0	+	+	+	/	+	/	/
	π	-	/	/	/	/	/	/

\mathbf{L}_N , while the second spin is negligible, with the single exception of a particular value of the quadrupolar parameter of a spinning neutron star or boson star in a binary with comparable masses. The details are summarized in Table III.

Coplanar configurations (of the spin vectors and orbital angular momentum) also allow for fixed points. We discussed the linear stability of them in the parameter plane of the spin polar angles, fixing all other parameters with the exception of the monotonously decreasing \tilde{I}_r , during the inspiral, the different values of which were represented as level curves. We reproduced earlier results holding for gravastar binaries. We also investigated the linear stability of black hole, neutron star, and boson star binaries, also of mixed black hole - gravastar, black hole - neutron star, and black hole - boson star binaries. In the particular numerical examples discussed, we found that

instabilities occur only for the gravastar - gravastar, boson star - boson star, and black hole - boson star binaries.

Our analysis highlights that the marginal stability of the spin configurations strongly depends on the value of the quadrupolar parameter, as shown in Figs. 4–7. We illustrate this statement in Table IV for four particular coplanar configurations. Any configuration in the (κ_1, κ_2) parameter plane could be marginally stable only for the corresponding value of \tilde{I}_r , represented by level curves. Fixing \tilde{I}_r (for example the blue curve), in other words picking a particular phase of the inspiral and the value of κ_1 in Figs. 4–7 allows us to read the value(s) of κ_2 of the marginally stable configuration at the respective phase of the inspiral.

The stability region is much larger for neutron star binaries than for black hole binaries in the coplanar configuration. Finally, the mixed systems exhibit a restricted stability parameter region.

ACKNOWLEDGMENTS

This work was supported by the Hungarian National Research Development and Innovation Office (NKFIH) in the form of Grant No. 123996 and has been carried out in the framework of COST actions CA16104 (GWverse) and CA18108 (QG-MM) supported by COST (European Cooperation in Science and Technology). Z. K. was further supported by the János Bolyai Research Scholarship of the Hungarian Academy of Sciences and by the ÚNKP-20-5–New National Excellence Program of the Ministry for Innovation and Technology through its National Research, Development and Innovation Fund.

[1] LIGO Scientific and Virgo Collaborations, GWTC-1: A Gravitational-Wave Transient Catalog of Compact Binary Mergers Observed by LIGO and Virgo during the First and Second Observing Runs, *Phys. Rev. X* **9**, 031040 (2019).

[2] <https://gracedb.ligo.org/latest/>.

[3] LIGO Scientific and Virgo Collaborations, GW170817: Observation of Gravitational Waves from a Binary Neutron Star Inspiral, *Phys. Rev. Lett.* **119**, 161101 (2017).

- [4] LIGO Scientific and Virgo Collaborations, GW190814: Gravitational waves from the coalescence of a 23 solar mass black hole with a 2.6 solar mass compact object, *Astrophys. J. Lett.* **896**, L44 (2020).
- [5] T. Damour and N. Deruelle, General relativistic celestial mechanics of binary systems. I. The post-Newtonian motion, *Ann. Inst. Henri Poincaré (Phys. Théor.)* **43**, 107 (1985).
- [6] L. Blanchet, Gravitational radiation from post-Newtonian sources and inspiralling compact binaries, *Living Rev. Relativity* **17**, 2 (2014).
- [7] B. M. Barker and R. F. O’Connell, Derivation of the equations of motion of a gyroscope from the quantum theory of gravitation, *Phys. Rev. D* **2**, 1428 (1970).
- [8] B. M. Barker and R. F. O’Connell, Gravitational two-body problem with arbitrary masses, spins, and quadrupole moments, *Phys. Rev. D* **12**, 329 (1975).
- [9] B. M. Barker and R. F. O’Connell, The gravitational interaction: Spin, rotation, and quantum effects—a review, *Gen. Relativ. Gravit.* **11**, 149 (1979).
- [10] L. E. Kidder, C. M. Will, and A. G. Wiseman, Spin effects in the inspiral of coalescing compact binaries, *Phys. Rev. D* **47**, R4183 (1993).
- [11] L. E. Kidder, Coalescing binary systems of compact objects to (post)^{5/2}-Newtonian order. V. Spin effects, *Phys. Rev. D* **52**, 821 (1995).
- [12] R. Rieth and G. Schäfer, Spin and tail effects in the gravitational-wave emission of compact binaries, *Classical Quant. Grav.* **14**, 2357 (1997).
- [13] L. Á. Gergely, Z. I. Perjés, and M. Vasúth, Spin effects in gravitational radiation backreaction III. Compact binaries with two spinning components, *Phys. Rev. D* **58**, 124001 (1998).
- [14] L. Á. Gergely, Spin-spin effects in radiating compact binaries, *Phys. Rev. D* **61**, 024035 (1999).
- [15] L. Á. Gergely, Second post-Newtonian radiative evolution of the relative orientations of angular momenta in spinning compact binaries, *Phys. Rev. D* **62**, 024007 (2000).
- [16] A. Klein and P. Jetzer, Spin effects in the phasing of gravitational waves from binaries on eccentric orbits, *Phys. Rev. D* **81**, 124001 (2010).
- [17] A. Buonanno, G. Faye, and T. Hinderer, Spin effects on gravitational waves from inspiraling compact binaries at second post-Newtonian order, *Phys. Rev. D* **87**, 044009 (2013).
- [18] E. Poisson, Gravitational waves from inspiraling compact binaries: The quadrupole-moment term, *Phys. Rev. D* **57**, 5287 (1998).
- [19] L. Á. Gergely and Z. Keresztes, Gravitational radiation reaction in compact binary systems: Contribution of the quadrupole-monopole interaction, *Phys. Rev. D* **67**, 024020 (2003).
- [20] B. Mikóczy, M. Vasúth, and L. Á. Gergely, Self-interaction spin effects in inspiralling compact binaries, *Phys. Rev. D* **71**, 124043 (2005).
- [21] É. Racine, Analysis of spin precession in binary black hole systems including quadrupole-monopole interaction, *Phys. Rev. D* **78**, 044021 (2008).
- [22] L. Á. Gergely, Spinning compact binary inspiral: Independent variables and dynamically preserved spin configurations, *Phys. Rev. D* **81**, 084025 (2010).
- [23] L. Á. Gergely, Spinning compact binary inspiral. II. Conservative angular dynamics, *Phys. Rev. D* **82**, 104031 (2010).
- [24] L. Á. Gergely and Z. Keresztes, Spinning compact binary dynamics and chameleon orbits, *Phys. Rev. D* **91**, 024012 (2015).
- [25] P. C. Peters, Gravitational Radiation and the Motion of Two Point Masses, *Phys. Rev.* **136**, B1224 (1964).
- [26] Z. Keresztes, M. Tápai, and L. Á. Gergely, preceding paper, Spin and quadrupolar effects in the secular evolution of precessing compact binaries with black hole, neutron star, gravastar or boson star components, *Phys. Rev. D* **103**, 084024 (2021).
- [27] N. Uchikata, S. Yoshida, and P. Pani, Tidal deformability and I-Love-Q relations for gravastars with polytropic thin shells, *Phys. Rev. D* **94**, 064015 (2016).
- [28] W. G. Laarakkers and E. Poisson, Quadrupole moments of rotating neutron stars, *Astrophys. J.* **512**, 282 (1999).
- [29] M. Urbanec, J. C. Miller, and Z. Stuchlik, Quadrupole moments of rotating neutron stars and strange stars, *Mon. Not. R. Astron. Soc.* **433**, 1903 (2013).
- [30] F. D. Ryan, Spinning boson stars with large self-interaction, *Phys. Rev. D* **55**, 6081 (1997).
- [31] J. D. Schnittman, Spin-orbit resonance and the evolution of compact binary systems, *Phys. Rev. D* **70**, 124020 (2004).
- [32] A. Gupta and A. Gopakumar, Probing evolution of binaries influenced by the spin-orbit resonances, *Classical Quant. Grav.* **31**, 105017 (2014).
- [33] D. Gerosa, M. Kesden, R. O’Shaughnessy, A. Klein, E. Berti, U. Sperhake, and D. Trifiro, Precessional Instability in Binary Black Holes with Aligned Spins, *Phys. Rev. Lett.* **115**, 141102 (2015).